An Equivalent Transmission-Line Model Containing Dispersion for High-Speed Digital Lines—With an FDTD Implementation

Alberto Scarlatti and Christopher L. Holloway, *Member, IEEE*

***Abstract*—The increase in processor speeds in the last few years has created a growing need for the accurate characterization of waveform propagation on lossy printed-circuit-board (PCB) transmission lines. Due to the dispersive nature of pulse propagation on lossy transmission lines, approximations of the classic transmission-line model can fail in this application (i.e., lossless or dc losses approximations). This paper will show how an equivalent-transmission-line model can be used to analyze dispersive transmission lines for high-speed digital applications. The equivalent-circuit elements of this transmission-line model incorporate the frequency dependence of the per unit length impedance and admittance caused by the finite conductivity of the conductors as well as the dielectric losses. We will show that these equivalent circuit elements can be readily implemented into finite-difference time-domain (FDTD) transmission-line codes, and we will present such a FDTD implementation. S-parameters and pulsed waveforms for a circular wire, coplanar waveguides (CPW) and microstrip lines are shown. Finally, we present approximate expressions for analytically obtaining the resistance and inductance per length of a microstrip line.**

***Index Terms*—Equivalent transmission-line model, FDTD, frequency dependent parameters, high-speed digital lines, lossy lines, signal integrity.**

I. Introduction

THE increase in processor speeds in the last few years has resulted in faster pulses on printed-circuit-board (PCB) transmission-line structures. Faster pulses imply higher frequency content than the electromagnetic compatibility (EMC) community has been concerned with in the past. Changes in high-frequency propagation characteristics can have an adverse effect on signal integrity in high-speed digital lines. This has spawned a growing need to understand and accurately characterize the propagation of high-frequency waveforms on transmission-line structures for signal integrity issues.

There are various techniques used to investigate frequency-dependent transmission-line parameters [1]–[18]. These include lumped-element approximations, equivalent-transmission-line models, the method of characteristics, closed-form approximations, and time-domain Green's function. In this paper we will concentrate on the use of an equivalent-transmission-line model where the transmission line parameters are approximated by Debye rational functions. It is illustrated how this equivalent-transmission-line model (i.e., the first-order Debye form) is well suited for easy implementation into finite-difference time-domain (FDTD) transmission-line codes. Details of the FDTD implementation are presented here.

The conventional approach to analyzing propagation on transmission lines is to use the classic transmission-line model, and the telegrapher's equations or transmission-line equations [19]–[22]

$$\frac{\partial V}{\partial z} = -ZI$$
$$\frac{\partial I}{\partial z} = -YV. \tag{1}$$

Z and Y represent, respectively, the distributed series impedance and shunt admittance p.u.l. of the line and are defined as

$$Z = R + j\omega L \quad \text{and} \quad Y = G + j\omega C \tag{2}$$

where $R(\Omega/m), L(H/m), C(F/m)$, and $G(S/m)$ represent, respectively, the per unit length (p.u.l.) series resistance, series inductance, shunt capacitance and shunt conductance. In general, all four of the transmission-line parameters are frequency dependent [21]. The frequency-dependent nature of R, L, C, and G causes time-domain high-speed digital waveforms to alter their shape when propagating along a dispersive transmission line.

A multiplication in the frequency-domain corresponds to a convolution in the time-domain, i.e.,

$$\frac{\partial v(z,t)}{\partial z} = -\mathcal{Z}(t) * i(z,t)$$
$$\frac{\partial i(z,t)}{\partial z} = -\mathcal{Y}(t) * v(z,t) \tag{3}$$

where $*$ represents a convolution integration; $\mathcal{Z}(t)$ and $\mathcal{Y}(t)$ are respectively the inverse Fourier transforms of the distributed p.u.l. series impedance and shunt admittance given in (2).

Because of this convolution and the impulsive nature of $\mathcal{Z}(t)$ and $\mathcal{Y}(t)$, an exact time-domain circuit model for dispersion is difficult; hence, approximations are usually used. One such approximation that is typically used can be thought of as a low-frequency model. In this model, R and L are assumed to be independent of frequency, where

$$R = R_{\text{dc}} \quad \text{and} \quad L = L_0 \tag{4}$$

Manuscript received August 18, 2000; revised August 30, 2001.

A. Scarlatti is with the Department of Electrical Engineering, University of Rome "La Sapienza", Rome 00184, Italy (e-mail: scarlatti@elettrica.ing.uniroma1.it).

C. L. Holloway is with the Radio-Frequency Technology Division, National Institute of Standards and Technology, U.S. Department of Commerce, Boulder Laboratories, Boulder, CO 80303 USA(e-mail: holloway@boulder.nist.gov).

Publisher Item Identifier S 0018-9375(01)10223-1.

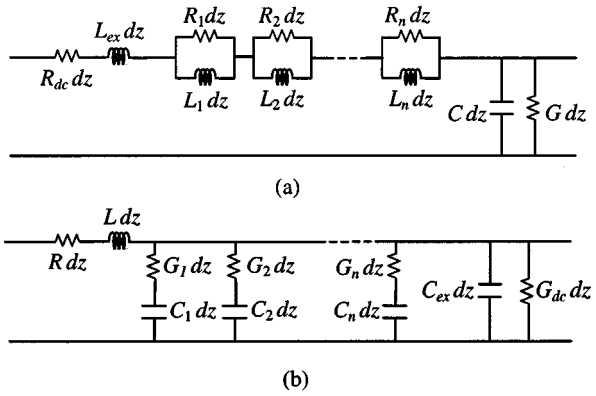

Fig. 1. Equivalent circuit of the dz-long transmission line: (a) representation of frequency dependent R and L, (b) representation of frequency dependent G and C.

where $R_{\rm dc}$ is the dc resistance p.u.l. of the line and L_0 is the dc inductance consisting of the external and internal inductance p.u.l. of the line. On some occasions the internal part is neglected. With these frequency-independent quantities, the transmission-line equations have the following time-domain form:

$$\frac{\partial v(z,t)}{\partial z} = -R_{\rm dc} i(z,t) - L_0 \frac{\partial i(z,t)}{\partial t}$$
$$\frac{\partial i(z,t)}{\partial z} = -G v(z,t) - C \frac{\partial v(z,t)}{\partial t}. \tag{5}$$

This low-frequency model cannot accurately take into account the dispersion of high-speed digital signals with significant high-frequency content.

Due to the smooth behavior of the frequency dependent $R, L, G,$ and C, a Debye rational approximation can be easily obtained for the quantities with a small number of poles. The equivalent-circuit model shown in Fig. 1 has this type of first-order Debye representation for the distributed transmission-line parameters. This equivalent transmission line is obtained by replacing the p.u.l. parameters of a standard transmission-line model with a series of a RL parallel network and a CG series network. The RL parallel network represented in Fig. 1(a) corresponds to a model where only frequency-dependent p.u.l. resistance and inductance (R and L) of the transmission line are considered, while the CG series network represented in Fig. 1(b) corresponds to a model where only frequency-dependent p.u.l. capacitance and conductance (G, i.e., dielectric loss and C) are considered. By combining these two models we can analyze the frequency-dependence of all four transmission-line parameters. This first-order Debye representation for the distributed transmission-line parameters is analogous to the classical approach of analyzing pulse propagation through lossy materials in which a series of first-order Debye terms are used for frequency dependent permittivity ϵ and permeability μ, see [14] and [23]–[27].

This type of first-order Debye representation for p.u.l. series resistance and inductance was first introduced in [1]. In this virtually unknown Russian publication, Gumerova, Efimov, and Kostenko [1] discussed how the RL parallel network portion of this equivalent-circuit network could be used for analyzing low-frequency propagation of atmospheric discharge on a transmission line over a lossy ground which incorporated dispersion effects due to the lossy ground. As discussed below, the work in [1] is connected to the approach presented in [2] and [3], and is the basis of the work in [4]. Other types of equivalent-circuit models have been used in the past to represent frequency-dependent parameters [5]–[9] (as discussed below). While higher-order rational function approximations are possible, it will be shown that the use of a first-order Debye form results in only a slight modification to the standard telegrapher's equations. Hence, this equivalent-transmission-line model (i.e., the first-order Debye form) gives rise to more effective implementation into FDTD transmission-line codes.

In this paper, we concentrate our efforts on frequency-dependent R and L resulting from field penetration into the conductors; hence only the equivalent-circuit model in Fig. 1(a) will be used for the example presented here. The network of L_i and R_i shown in this figure allows for the distributed per unit length parameters of the line to be expressed as the following:

$$R = R_{\rm dc} + \omega^2 \sum_{i=1}^{N} \frac{L_i^2/R_i}{1 + \left(\frac{\omega L_i}{R_i}\right)^2} \tag{6}$$

$$L = L_{\rm ext} + \sum_{i=1}^{N} \frac{L_i}{1 + \left(\frac{\omega L_i}{R_i}\right)^2} \tag{7}$$

and

$$Z = R + j\omega L \tag{8}$$

or

$$Z = R_{\rm dc} + j\omega L_{\rm ext} + j\omega \sum_{i=1}^{N} \frac{L_i}{1 + j\omega \frac{L_i}{R_i}} \tag{9}$$

where $R_{\rm dc}$ is defined above and $L_{\rm ext}$ is the external inductance. Note that the internal inductance $L_{\rm int}$ is given by

$$L_{\rm int} = \sum_{i=1}^{N} L_i. \tag{10}$$

This formulation can be used to approximate the exact values for R and L. In doing so, we must choose the number of poles N and determine the corresponding R_i and L_i. In determining these parameters, we assumed that both R and L of the transmission-line structure are known. These reference values can be obtained from analytic expression, measurement data, and/or full-wave numerical modeling. Once R and L are known, then R_i and L_i for a given N are obtained by an optimization procedure which matches (9) to the known per unit length line impedance along the desired frequency range, as discussed in Section III. If the frequency-dependent C and G of a transmission line are desired, the network model shown in Fig. 1(b) results in a similar set of Debye equations for Y

$$G = G_{\rm dc} + \omega^2 \sum_{i=1}^{N} \frac{C_i^2/G_i}{1 + \left(\frac{\omega C_i}{G_i}\right)^2} \tag{11}$$

$$C = C_{\rm ext} + \sum_{i=1}^{N} \frac{C_i}{1 + \left(\frac{\omega C_i}{G_i}\right)^2} \tag{12}$$

and

$$Y = C + j\omega G \tag{13}$$

or

$$Y = G_{\rm dc} + j\omega C_{\rm ext} + j\omega \sum_{i=1}^{N} \frac{C_i}{1 + j\omega \frac{C_i}{G_i}}. \tag{14}$$

The formulation presented in (9) assures that the dc values of R and L are captured. On the other hand, the $\sqrt{f}$ behavior of R and the $1/\sqrt{f}$ behavior of L are not guaranteed with this Debye model. However, the high-frequency accuracy of this approximation improves with increasing number of poles N (as shown below).

The present paper illustrates how this type of model can be used to determine the S-parameters and pulsed waveforms for different types of planar transmission-line structures used for PCB's. Results for circular wire lines, coplanar waveguides (CPW), and microstrip lines will be presented. We should note that rational functions for representing transfer functions of transmission lines (9) have been used in the past [2]–[5]. In fact, the use of a series of first-order Debye terms that fall out of this circuit model is the basis of the so-called W-element approach [2] and [3]. This illustrates that the model discussed in the paper, together with [1], gives a circuit interpretation of the W-element.

Alternative types of equivalent-circuit, skin-effect models have been used in the past to represent frequency-dependent parameters [5]–[9], dating back to Wheeler's work on formulas for the skin effect in the 40's [10]. The models presented in [6] [7]–[9] are referred to as the ladder model. It can be shown that the ladder model results in rational function approximations for R and L as well. The higher-order rational functions that result from the ladder model can be implemented in FDTD transmission-line codes with convolution integral approaches. The alternative circuit model presented in this paper (i.e., a series of first-order Debye terms) allows for an alternative FDTD formulation that is analogous to the magnetic susceptibility term used in an FDTD model of lossy magnetic ferrite materials [27], as shown in the next section. This alternative FDTD formulation results in a series of first-order differential equations, while the ladder model results in higher-order differential equations (or even integro-differential equations for some rational functions) that must be solved. As the number of circuit elements in the ladder model increase so does the order of the differential equation, which adds to the complexity. On the other hand, as the number of circuit elements increase in the Debye model, we need only to add additional first-order equations. In fact, below it is shown that the use of first-order Debye terms results in a set of equations that are equivalent to the standard telegrapher's transmission-line equations. While higher-order rational functions can be implemented into FDTD code, the resulting equations require higher-order derivatives, and as a result the simple connection to the standard telegrapher's transmission-line equations is not possible. With this said, a connection exists between the higher-order rational function, used in the ladder model, and the series of first-order Debye terms used in this model. Recall that many higher-order rational function can be re-expressed as a series of first-order Debye terms. Thus, the model presented here gives an alternative circuit-model interpretation of dispersion that can be easily incorporated into FDTD transmission-line models.

Details of the FDTD implementation are presented here. Once the FDTD procedure is introduced, S-parameters and pulsed waveforms for circular wire lines, CPW, and microstrip lines will be presented. We also show that the use of three to four terms in the Debye model is all that is required to accurately model the frequency-dependent parameters over the frequency range of interest.

This equivalent-transmission-line model requires the knowledge of the frequency dependent p.u.l. transmission-line parameters (for example, R and L). These parameters can be obtained from either measured data, analytic results, and/or full-wave numerical results. Once the transmission-line parameters are known and the constant needed for the Debye rational fit are determined, it is then possible to analyze pulse propagation. The examples shown in this paper are based on transmission-line parameters obtained from measured data, analytic results, and/or full-wave numerical results.

II. Finite-Difference Time-Domain (FDTD) Implementation of the Equivalent Transmission-Line Model

The procedure for incorporating this circuit-model (i.e., a series of first-order Debye terms) into a FDTD transmission-lines code is very similar to the manner in which Debye models for lossy magnetic ferrite materials have been implemented into FDTD codes [27]. We will first show the procedure for one first-order Debye term and then generalize to N first-order Debye terms. Start by rewriting the first expression in (1) as

$$\frac{\partial V(\omega, z)}{\partial z} = -j\omega L_{\rm ext} B \tag{15}$$

where

$$B = \left[\frac{R_{\rm dc}}{j\omega L_{\rm ext}} + \frac{L_1}{L_{\rm ext}} \frac{1}{1 + j\omega \frac{L_1}{R_1}} + 1 \right] I. \tag{16}$$

Rewriting (15) in the time-domain, the following expression relates V and B:

$$\frac{\partial v(z,t)}{\partial z} = -L_{\rm ext} \frac{\partial b(z,t)}{\partial t}. \tag{17}$$

By using a standard staggered space and time grid, the following update equation for the discretized $b(k)^n$ is obtained

$$b(k)^{n+1} = b(k)^n - \frac{\Delta t}{L_{\rm ext} \Delta z} \left[v(k+1)^{n+1/2} - v(k)^{n+1/2} \right] \tag{18}$$

where it is assumed $z = k\Delta z$ and $t = n\Delta t$. With this value of $b(k)^{n+1}$ and (16), an update expression for $i(k)^{n+1}$ can be obtained in the discretized time-domain.

Rewrite (16) as

$$B = I + D + M \tag{19}$$

where

$$D = \frac{R_{\rm dc}}{j\omega L_{\rm ext}} I \tag{20}$$

$$M = \frac{L_1}{L_{\rm ext}} \left(\frac{1}{1 + j\omega \frac{L_1}{R_1}} \right) I. \tag{21}$$

Note that

$$D + M = \chi I \tag{22}$$

where χ is analogous to the magnetic susceptibility used in lossy materials [27], and is given by

$$\chi = \frac{R_{\rm dc}}{L_{\rm ext}} \frac{1}{j\omega} + \frac{L_1}{L_{\rm ext}} \left(\frac{1}{1 + j\omega \frac{L_1}{R_1}} \right). \tag{23}$$

Solving (20) for I and comparing to (19) yields

$$j\omega \frac{L_{\rm ext}}{R_{\rm dc}} D = B - D - M. \tag{24}$$

Equation (24) is transformed in the time-domain giving

$$\frac{L_{\rm ext}}{R_{\rm dc}} \frac{\partial d(z,t)}{\partial t} + d(z,t) + m(z,t) = b(z,t). \tag{25}$$

An expression for the updating of both $d(k)^n$ and $m(k)^n$ can be obtained by using standard center-difference schemes

$$\mathcal{A} d(k)^{n+1} + m(k)^{n+1} = RS1 \tag{26}$$

where

$$\mathcal{A} = \left[\frac{2L_{\rm ext}}{R_{\rm dc} \Delta t} + 1 \right] \tag{27}$$

and $RS1$ represents all the known values of the previous time-step

$$RS1 = b(k)^{n+1} + b(k)^n + \left[\frac{2L_{\rm ext}}{R_{\rm dc} \Delta t} - 1 \right] d(k)^n - m(k)^n. \tag{28}$$

In a similar manner, solving (21) for I and comparing to (19) results in

$$\frac{L_{\rm ext}}{L_1} \left[1 + j\omega \frac{L_1}{R_1} \right] M = B - D - M \tag{29}$$

which is rewritten in the time-domain as

$$\left[\frac{L_{\rm ext}}{L_1} + 1 \right] m(z,t) + \frac{L_{\rm ext}}{R_1} \frac{\partial m(z,t)}{\partial t} + d(z,t) = b(z,t). \tag{30}$$

By using standard center-difference schemes on the equation, the needed second expression for the updating of $d(k)^n$ and $m(k)^n$ is obtained

$$d(k)^{n+1} + \mathcal{Q} m(k)^{n+1} = RS2 \tag{31}$$

where

$$\mathcal{Q} = \left[\frac{2L_{\rm ext}}{R_1 \Delta t} + \frac{L_{\rm ext}}{L_1} + 1 \right] \tag{32}$$

and $RS2$ represents the known terms

$$RS2 = b(k)^{n+1} + b(k)^n + \left[\frac{2L_{\rm ext}}{R_1 \Delta t} - \frac{L_{\rm ext}}{L_1} - 1 \right] m(k)^n - d(k)^n. \tag{33}$$

Equations (26) and (31) must be solved simultaneously to give $d(k)^{n+1}$ and $m(k)^{n+1}$. Finally, the update expression for $i(k)^{n+1}$ is obtained from (19)

$$i(k)^{n+1} = b(k)^{n+1} - d(k)^{n+1} - m(k)^{n+1}. \tag{34}$$

Once $i(k)^{n+1}$ is determined, a standard FDTD staggered space-time scheme can be applied to the second expression in (1) to obtain the following update for $v(k)^{n+3/2}$:

$$v(k)^{n+3/2} = v(k)^{n+1/2} - \frac{\Delta t}{C \Delta z} \left[i(k)^{n+1} - i(k-1)^{n+1} \right]. \tag{35}$$

A set of updating equations for the FDTD scheme can be defined as

$$\begin{aligned}
b(k)^{n+1} &= b(k)^n - \frac{\Delta t}{L_{\rm ext} \Delta z} \left[v(k+1)^{n+1/2} - v(k)^{n+1/2} \right] \\
d(k)^{n+1} &= \frac{1}{\mathcal{A}\mathcal{Q} - 1} \left[\mathcal{Q} RS1 - RS2 \right] \\
m(k)^{n+1} &= \frac{1}{\mathcal{A}\mathcal{Q} - 1} \left[\mathcal{A} RS2 - RS1 \right] \\
i(k)^{n+1} &= b(k)^{n+1} - d(k)^{n+1} - m(k)^{n+1} \\
v(k)^{n+3/2} &= v(k)^{n+1/2} - \frac{\Delta t}{C \Delta z} \left[i(k)^{n+1} - i(k-1)^{n+1} \right].
\end{aligned} \tag{36}$$

Thus, we see that the first-order Debye approximation for the frequency-dependent parameters gives a set of equations that are very similar to the discretized classical telegrapher's transmission-line equations. It can also be shown that a similar set of equations are obtained for the equivalent-circuit model shown in Fig. 1(b) (i.e., the model for frequency-dependent C and G).

Note that (26) and (31) can be rewritten as an unique equation by defining the new variable

$$M' = D + M. \tag{37}$$

However, this can only be done at the expense of requiring a second-order time derivative approximation when solving for M'.

The procedure above can be generalized to N first-order Debye terms, in which B is re-expressed as

$$B = I + D + \sum_{i=1}^{N} M_i \tag{38}$$

where

$$\begin{aligned}
D &= \frac{R_{\rm dc}}{j\omega\, L_{\rm ext}} I \\
M_i &= \left[\frac{L_i}{L_{\rm ext}} \frac{1}{1 + j\omega \frac{L_i}{R_i}} \right] I \quad \text{for } i = 1, 2, \ldots N.
\end{aligned} \tag{39}$$

These expressions represent a set of $N+1$ equations, resulting from the D term and N different M_i terms, all written in terms of I. However, I is as yet unknown and a procedure similar to the above is used to eliminate I, i.e., $I = B - D - \sum_{i=1}^{N} M_i$. We are left with $N+1$ equations that can be solved simultaneously via matrix inversion to obtain an update expression for $d(k)^n$ and each of the $m(k)_i^n$'s. Once $d(k)^n$ and the $m(k)_i^n$'s are obtained the update expression for $i(p)^{n+1}$ is

$$i(k)^{n+1} = b(k)^{n+1} - d(k)^{n+1} - \sum_{i=1}^{N} m(k)_i^{n+1}. \qquad (40)$$

Like all numerical approaches, in order to get accurate results with this FDTD implementation, the transmission line must be divided into at least 10 cells per wavelength of the maximum frequency of interest.

III. Debye Approximation Procedure

In representing the frequency-dependent behavior of a transmission line by the model shown in Fig. 1(a), the number N of Debye terms and the unknown parameters R_i and L_i must be chosen. The number N of Debye terms is related to the number of poles of the rational function expressed by (9) used to approximate the per unit length impedance of the line. It will be shown by numerical experimentation that a good matching for different types of transmission lines of fixed geometry along a frequency range reaching a few gigahertz is obtained using no more than three or four Debye terms. The relatively few number of terms provides an extremely simple model. Moreover, a three or four Debye terms rational function can be easily optimized to match the smooth real and imaginary parts of the per unit length impedance of the line. This can be done using a simple minimum least squares technique implemented in many commercial mathematical programs.

One needs to use caution and not blindly use optimizing routines. In particularly, care must be taken in order to obtain positive values for the Debye parameters L_i and R_i. This is accomplished by optimizing for a parameter x, where x is the square root of one of the unknowns (for example, $x^2 = L_i$). By this method the Debye coefficients represent physical quantities. While nonpositive values of R_i and L_i can results in acceptable fits to the frequency-dependent parameters, nonpositive values lead to problems. Finally, if the analysis is focused in the high frequency range, it could be useful to consider $R_{\rm dc}$ and $L_{\rm int}$ in the Debye terms as unknown parameters gaining a better high frequency match at the expense of the low frequency convergence.

The vector-fitting procedure as presented in [28] can also be used to determine the unknowns in the Debye approximation [4]. This vector-fitting procedure is more involved to implement, but on the other hand, if we were needing several terms in the rational approximation it would be the preferred choice. We have compared results from the vector-fitting procedure to those obtained using the simple least squares approaches and the results are very similar.

IV. Application of the Equivalent Transmission-Line Model to Different Transmission-Line Structures

In this section, the model is applied to three different transmission-line structures: a circular wire over a perfect conducting ground plane, a CPW line and a microstrip line. For the circular wire transmission line, the frequency-dependent R and L are known analytically. For the CPW line, R and L are obtained from a full-wave numerical solution; for the microstrip, R and L are obtained from both measured data and from approximate closed-form expressions. The time-domain results in this section are excited by the following Gaussian pulse

$$v(t) = V_0 \exp\left(-\kappa \frac{(t-\alpha)^2}{\alpha^2}\right) \qquad (41)$$

with $\alpha = 0.35$ ns, $\kappa = 10$ and peak value $V_0 = 1$ V. These choices of α and κ ensure that the pulse has a frequency spectra reaching a few gigahertz.

A. Circular Wire Over a Ground Plane

A circular wire over a perfect conducting ground plane with radius $a = 0.1$ mm, height $h = 25$ mm and characterized by a conductivity $\sigma = 5.8 \cdot 10^7$ S/m is depicted in the insert of Fig. 2. R and L for this geometry are known analytically [22] and are also shown in Fig. 2. With these known values of R and L, it is possible to determine the unknown constants in (6) and (7) for different values of N. These unknown constants are obtained by the optimization procedure described in the previous section. Fig. 2 gives values of R and L as defined from (9), for N equal to 1, 2, and 3. The convergence of the approximation curve to the exact solution can be improved by increasing the number N of Debye terms, and a good fit over eight decades of frequency is obtained using the $N = 3$ Debye model. Notice that the approximation for $N = 3$ agrees well with the analytical curve. Fig. 3 shows the error between the absolute values of Z and the approximated Debye functions. Again, there is good agreement.

B. CPW Line

A CPW line with $w = 73$ μm, $b = 49$ μm, $w_g = 250$ μm, $t = 0.5883$ μm, $h = 254$ μm, $\epsilon_r = 10$ and metal conductivity $\sigma = 3.37 \cdot 10^7$ S/m is depicted in the insert of Fig. 4. R and L for this geometry were obtained from a full-wave mode-matching procedure [17] and are shown as dots in Fig. 4. With these known values of R and L it is possible to determine the unknown constants in (6) and (7), for different values of N. Also shown in Fig. 4 are the approximate data for R and L, obtained from (9), for N equal to 1, 2, 3, and 4. Notice the good correlation obtained when $N \geq 3$. Fig. 5 compares the $|S_{12}|$ parameters for a 0.5 m long line, terminated at both ends with a resistance of 50 Ω, obtained from the dc approximation (R and L independent of frequency) and with the Debye models with different values of N. It is interesting to note that the behavior of the line is achieved by increasing the number of poles of the approximating function, as clearly shown in Fig. 5.

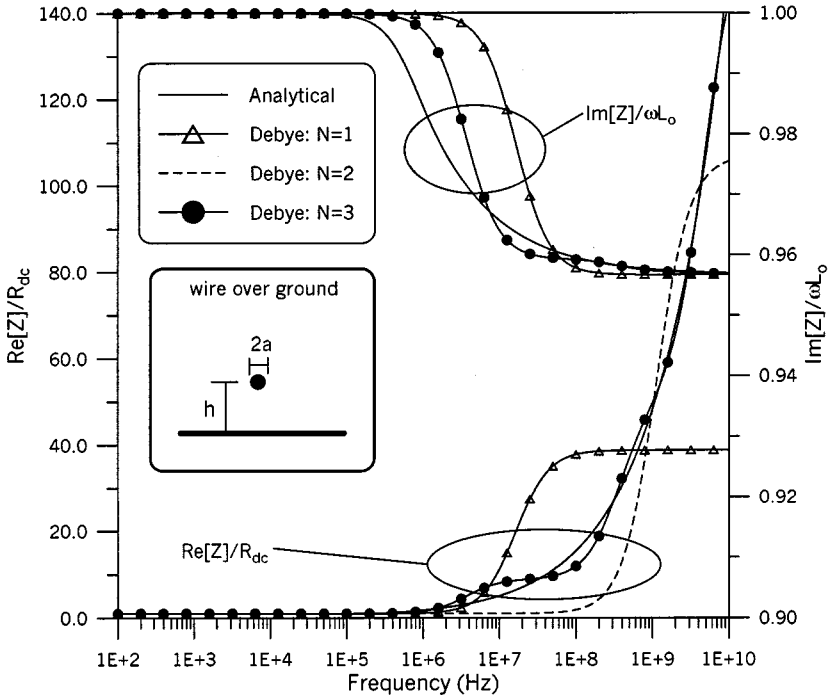

Fig. 2. R and L for a circular wire above a ground plane with $a = 0.1$ mm and $h = 25$ mm obtained from analytic results and from the Debye model.

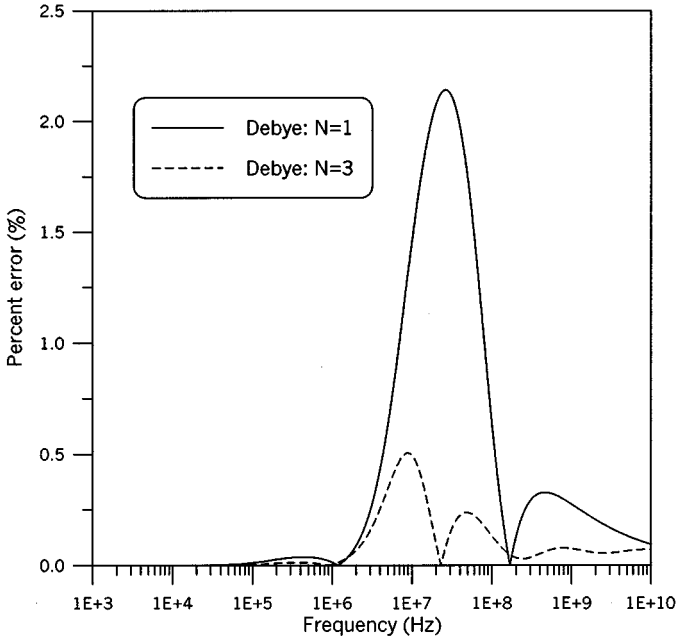

Fig. 3. Percent error of the absolute values of Z with respect to the analytic results for a circular wire above a ground plane with $a = 0.1$ mm and $h = 25$ mm.

Once the transmission-line parameters are obtained, pulse dispersion for a given length of line is investigated. Pulse propagation can be obtained by solving in the frequency-domain and inverse Fourier transforming the results. This is the frequency-domain to time-domain transformation method presented in [21]. The inverse Fourier transform approach was used to obtain the pulse shape at the far end of a line 0.5 m long and terminated at both ends with a resistance of 50 Ω, using the dc approximation and the Debye model with three values of N. These results are shown in Fig. 6. Notice that using three or four Debye terms does not greatly change the shape of the transmitted pulse confirming that three or four terms are enough to characterize the line in the interested frequency range. An alternative approach is to apply the FDTD procedure discussed in Section II. FDTD results for the transmitted pulse shape along the same line for two values of N are shown in Fig. 7. These figures compare the results of the inverse Fourier transform from a frequency-domain model with the application of the time-domain FDTD method. Note that both approaches (the frequency-domain model and the FDTD model) yield the same results for the same N-th order Debye model. This shows that implementing the FDTD model correctly models dispersion. Notice how the dc approximation does not correctly model dispersion.

Figs. 6 and 7 illustrate the effects of dispersion. The pulse is broadened and exhibits the classic late-time tail, seen in time-domain response of lossy media. From these figures we also see that the dc approximation is not adequate for this example. The pulse obtained from the dc approximation is larger in amplitude and narrower in width. Notice however, that all three results in these figures approach the same late-time values. This is due to the fact that the late-time response corresponds to low-frequency in the frequency-domain, and as seen from Fig. 5, all three cases (dc, $N = 1$, and $N = 3$) capture the same low-frequency frequency-dependent behavior. On the other hand, from Figs. 6 and 7, the early-time response (the front edge of the pulse) which corresponds to high-frequency in the frequency-domain is where three of the cases (dc, $N = 1$, and $N = 3$)

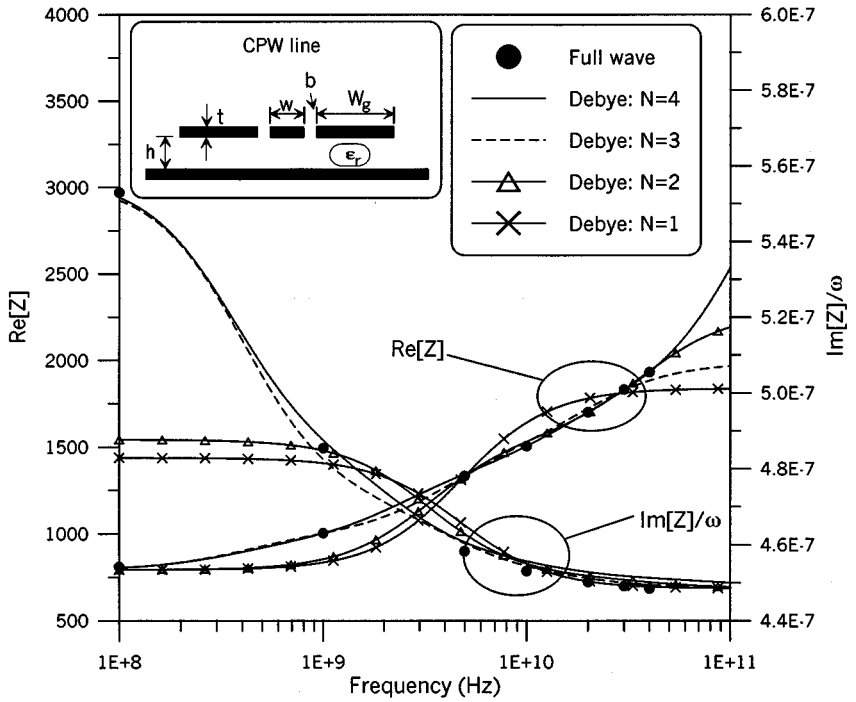

Fig. 4. R and L for a CPW line with $w = 73\ \mu$m, $t = 0.5883\ \mu$m, $w_g = 250\ \mu$m, $b = 49\ \mu$m, $h = 254\ \mu$m, $\sigma = 3.37 \cdot 10^7$ S/m and $\epsilon_r = 10$ obtained from numerical results and from the Debye model.

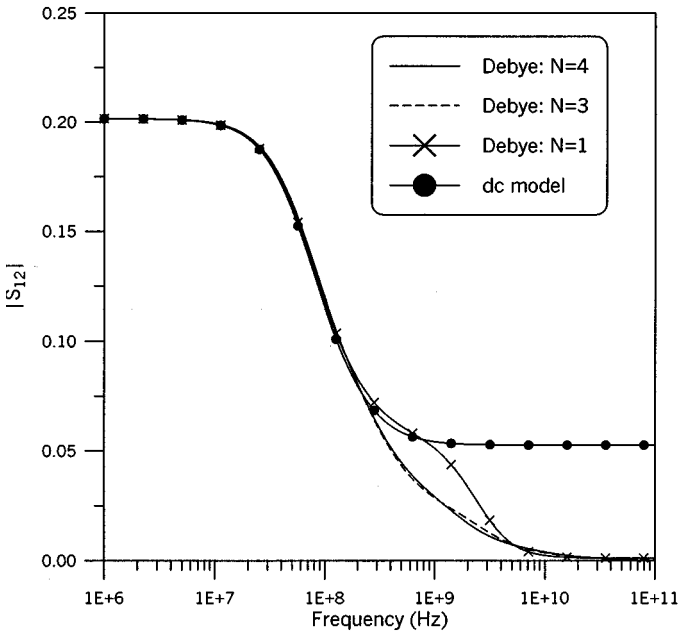

Fig. 5. Magnitude of S_{12} for a CPW line with $w = 73\ \mu$m, $t = 0.5883\ \mu$m, $w_g = 250\ \mu$m, $b = 49\ \mu$m, $h = 254\ \mu$m, $l = 0.5$ m, $\sigma = 3.37 \cdot 10^7$ S/m and $\epsilon_r = 10$ obtained from the dc approximation and from the Debye model.

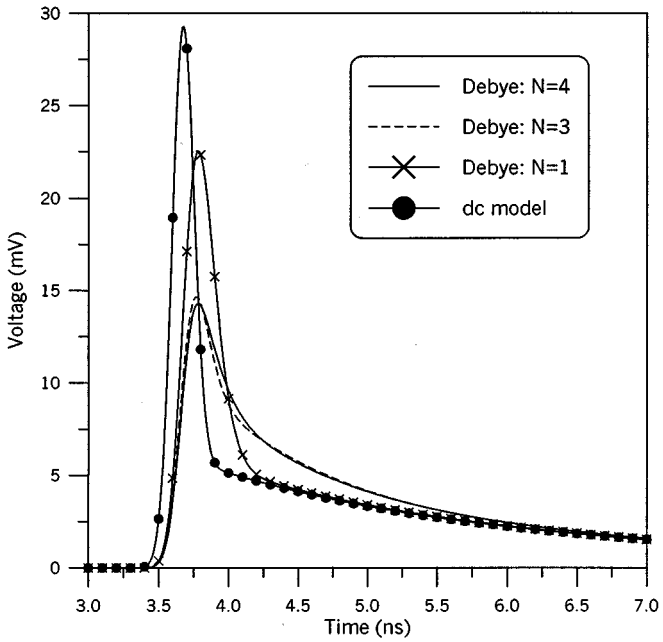

Fig. 6. The transmitted pulse shape for a CPW line with $w = 73\ \mu$m, $t = 0.5883\ \mu$m, $w_g = 250\ \mu$m, $b = 49\ \mu$m, $h = 254\ \mu$m, $l = 0.5$ m, $\sigma = 3.37 \cdot 10^7$ S/m and $\epsilon_r = 10$ obtained from Fourier transform approach.

differ. This is due to the fact that the frequency-dependent behavior for all three cases began to deviate from one another around 200 MHz, as seen in Fig. 5.

C. Microstrip Line

Two microstrip line geometries were analyzed. The insert of Fig. 8 shows a generic transverse cross-section. A microstrip line having $w = 105\ \mu$m, $t = 1.8\ \mu$m, $h = 254\ \mu$m, $\epsilon_r = 10$ and metal conductivity $\sigma = 3.3 \cdot 10^7$ S/m, is considered first. Data for R and L for this structure were obtained from the measurement procedure presented in [29] and [30]. With these known values of R and L we can determine the known constants in (6) and (7) for different values of N. Measured data for R plus approximated data obtained from the optimized Debye models

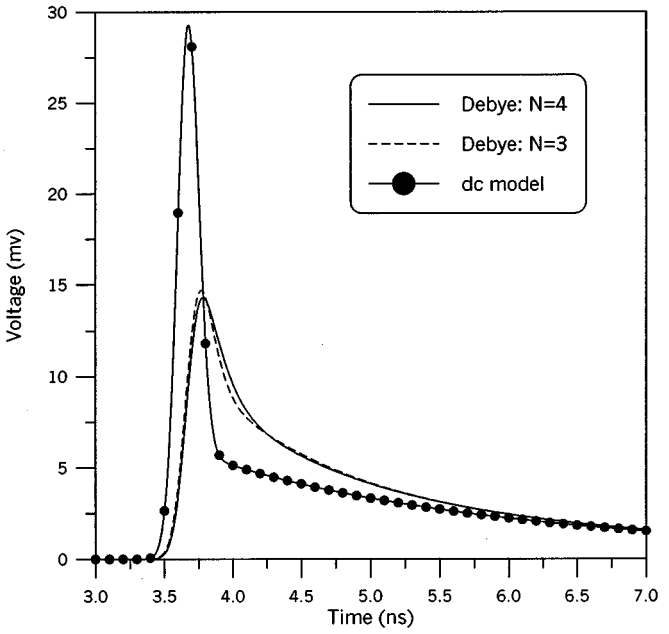

Fig. 7. The transmitted pulse shape for a CPW line with $w = 73\ \mu$m, $t = 0.5883\ \mu$m, $w_g = 250\ \mu$m, $b = 49\ \mu$m, $h = 254\ \mu$m, $l = 0.5$ m, $\sigma = 3.37 \cdot 10^7$ S/m and $\epsilon_r = 10$ obtained from the FDTD approach.

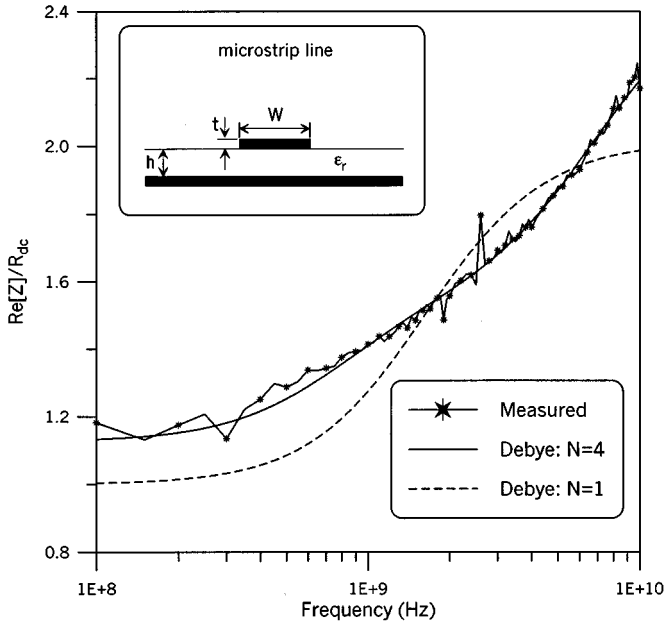

Fig. 8. R for a microstrip line with $w = 105\ \mu$m, $t = 1.8\ \mu$m, $h = 254\ \mu$m, $\sigma = 3.3 \cdot 10^7$ S/m and $\epsilon_r = 10$ obtained from the measured results and from the Debye model.

with $N = 1$ and $N = 4$ are shown in Fig. 8. Notice that the data for $N = 4$ agrees well with the measured data.

Measured data of R and L for arbitrary microstrip structures are not always available. Hence closed-form expressions for R and L are desirable. However, expressions for R and L that are valid over a large frequency range (i.e., dc to ten's of GHz) have not been readily available. Here, we will introduce approximate closed-form expressions for R and L that ensure the dc limits as well as the higher frequency limits.

In previous works [31]–[33], closed-form expressions for the attenuation constants for various planar structures were derived. These expressions have been shown to be valid for t/δ (t is the strip thickness and δ is the skin depth) on the order of 1 and greater. From these works, R per unit length, valid for $t/\delta \geq 1$, can be obtained from

$$R = 2Z_0\alpha \tag{42}$$

where Z_0 is the characteristic impedance of the line and α is the attenuation constant. From the previous expression and [31], R for a microstrip line is given by

$$R = \frac{R_{sm}}{w\pi^2}Q \tag{43}$$

where

$$Q = \ln\left(\frac{w}{\Delta} - 1\right) \tag{44}$$

and R_{sm} is a modified surface impedance that takes into account coupling between the top and bottom of the strip and is given in [31]. Δ is a parameter that is a function of edge shape, strip thickness, and skin depth, and is given in [31]–[33]. Unfortunately, due to the inherent assumptions made in the derivation of this expression, R does not reduce to the dc limit. R will vary monotonically from its dc value to the $\sqrt{f}$ behavior at higher frequency. Such a variation can be approximated by the following expression:

$$R_n = R + e^{\frac{-2t}{\delta}}\left[R_{\rm dc} - \frac{2}{t\sigma}Q\right] \tag{45}$$

where R is given in (43) and $R_{\rm dc} = 1/(wt\sigma)$. This expression assures that $R_{\rm dc}$ is obtained for small values of the skin depth. Expression (45) has been compared to the measured data in Fig. 8 with differences no larger than 4%. Comparisons to other structures show similar or better correlation.

An approximate expression for L has a similar form

$$L_n = L_{\rm ext} + L_{\rm int}e^{\frac{-2t}{\delta}} \tag{46}$$

where $L_{\rm ext}$ is the external inductance given in [34] and $L_{\rm int}$ is the dc internal inductance. Since approximate formulas for the internal inductance $L_{\rm int}$ of a microstrip line exist only for small aspect ratios, a numerical code is used for the calculation of its dc value [35]. The line impedance Z and admittance Y can now be approximated by the following expressions:

$$Z = R_n + j\omega L_n \tag{47}$$

and

$$Y = G + j\omega C_0 \tag{48}$$

where C_0 is given in [36].

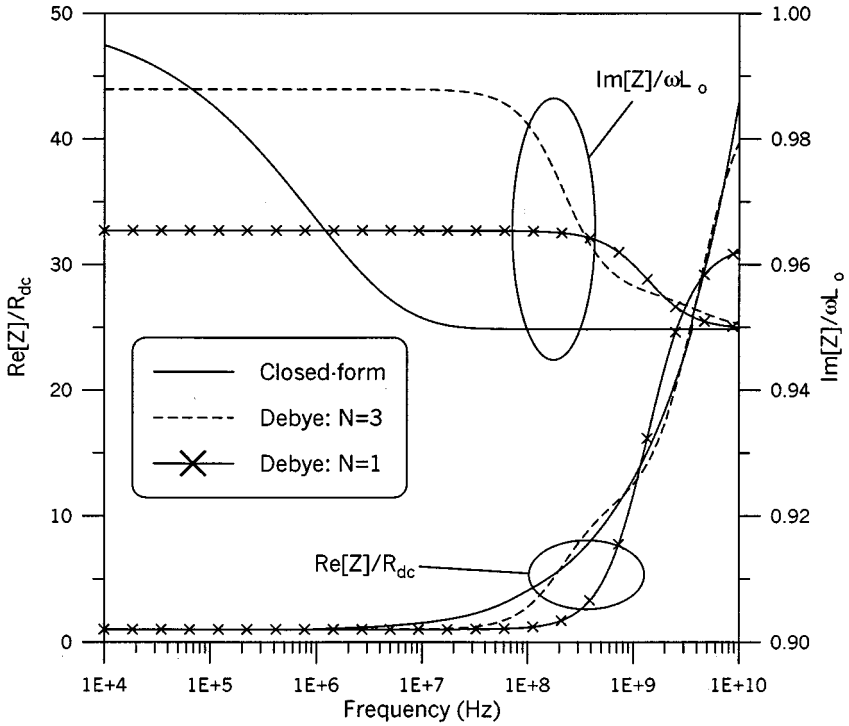

Fig. 9. R and L for a microstrip line with $w = 355.6\ \mu$m, $t = 35.05\ \mu$m, $h = 180\ \mu$m, $\sigma = 5.8 \cdot 10^7$ S/m and $\epsilon_r = 4.5$ obtained from the closed-form formulation and from the Debye model.

While the closed-form expressions given in (45) and (46) accurately predict the frequency-dependent behavior of R and L, they are not causal. Alternative causal closed-form expressions are found in [17], but, the expressions in [17] inaccurately predict the low-frequency inductance. However, by fitting the first-order Debye model to the expressions given in (45) and (46), we are not only insured a causal presentation for Z, but we are insured that the low-frequency behavior of R and L is captured.

A microstrip line having $w = 355.6\ \mu$m, $t = 35.05\ \mu$m, $h = 180\ \mu$m, $\epsilon_r = 4.5$ and conductivity of the metal strips $\sigma = 5.8 \cdot 10^7$ S/m, is considered. The line is $l = 1$ m long and is terminated at both ends with a resistance $R = 50\ \Omega$. This configuration is characterized by a dc internal inductance $L_{\text{int}} \simeq 1.575 \cdot 10^{-8}$ H/m. Fig. 9 shows R and L obtained by optimizing the Debye model for various N to the closed-form model given in (45) and (46). Note that the small relative difference between the imaginary part of Z for $N = 3$ Debye model and that of (46) still results in a good characterization of Z; below it is shown that the approximation leads to very good results for the transmitted waveforms. The approximation of L and R can be further improved if additional terms in the Debye model are used. Fig. 10 compares $|S_{12}|$ obtained from the closed-form model to the Debye model for two values of N. The Debye model data agree well with the reference results for $N \geq 3$.

FDTD results for transmitted pulse shapes at the far end of the line for various values of N are shown in Fig. 11. This figure compares the closed-form model, the dc approximation, and the Debye approximation. As expected, when N increases, the FDTD results approach the reference results. Once again, notice how poorly the dc approximation matches the exact solution for the pulse, due to its neglect of high-frequency content.

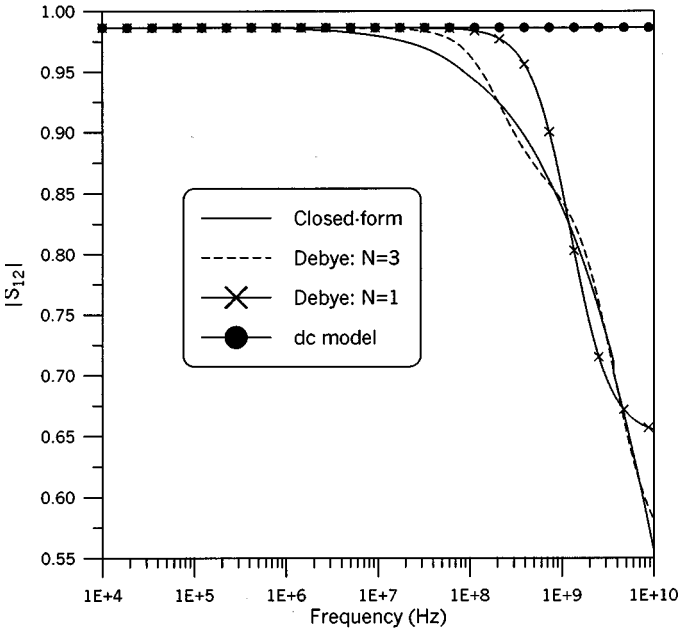

Fig. 10. Magnitude of S_{12} for a microstrip line with $w = 355.6\ \mu$m, $t = 35.05\ \mu$m, $h = 180\ \mu$m, $l = 1$ m, $\sigma = 5.8 \cdot 10^7$ S/m and $\epsilon_r = 4.5$ obtained from the closed-form formulation and from the Debye model.

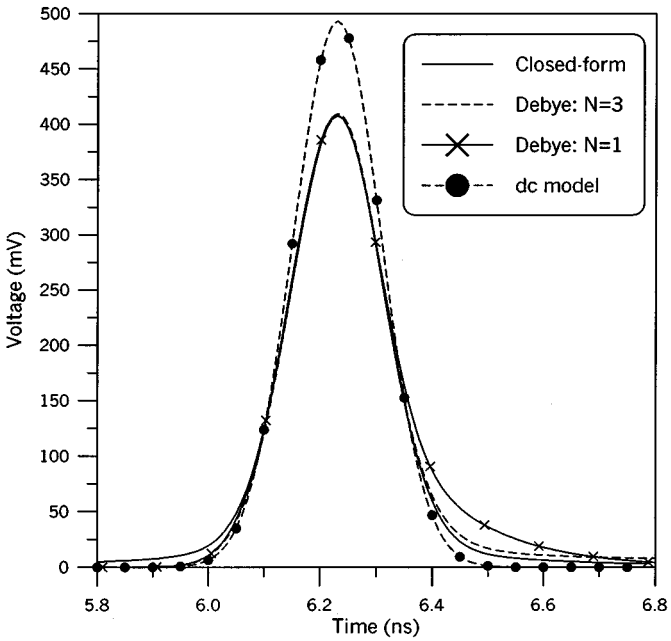

Fig. 11. The transmitted pulse shape for a microstrip line with $w = 355.6\ \mu$m, $t = 35.05\ \mu$m, $h = 180\ \mu$m, $l = 1$ m, $\sigma = 5.8 \cdot 10^7$ S/m and $\epsilon_r = 4.5$ obtained from the closed-form formulation and from the FDTD approach.

V. Conclusion

In this paper, we have illustrated how an equivalent-transmission-line model can be used to analyze dispersive transmission lines for high-speed digital applications. The intent of the model is that, once R and L are known, it can be used to characterize signal dispersion on transmission lines. Therefore, to effectively use this model one needs to know a priori the frequency-dependent transmission-line parameters R and L. These transmission-line parameters can be obtained by various means. We illustrated that this model can be used to accurately approximate the frequency-dependent parameters obtained from measured data, full-wave numerical data, and analytical models of R and L with the use of only three or four first-order Debye terms. Such a simple model can be used to investigate signal integrity for lossy transmission lines. Moreover the advantage of the circuit model presented here (i.e., a series of first-order Debye terms) is that it can be very easily incorporated into FDTD transmission-line codes used to solve pulse propagation. Such a procedure was presented. S-parameters and pulsed waveform outputs for circular wire, CPW, and microstrip lines were presented and compared to known results. Notice that the proposed method is suitable for time-domain analysis whenever nonlinear loads are connected to the line investigated. The simplicity of the Debye equivalent circuit transmission-line model allows for easy implementation into commercial circuit simulation solvers, such as SPICE. Both the FDTD and SPICE implementation require only a few seconds of run time, resulting in efficiency in analyzing pulse dispersion and signal integrity on lossy transmission lines.

This FDTD implementation of frequency-dependent transmission-line parameters can be applied to other problems besides PCB applications. Another very important application for this FDTD model is in electromagnetic coupling onto lossy cables onboard aircraft. Furthermore, the usefulness and importance of one-dimensional FDTD transmission-line models is illustrated in [37], where it is shown that simple one-dimensional FDTD transmission-line models can accurately predict the characteristics of pulse propagation on complicated PCB configurations when compared to full three-dimensional numerical models.

In the paper, we used the circuit model shown in Fig. 1(a) to investigate dispersion uniquely associated with frequency-dependent R and L. The effects of frequency-dependent C and G (i.e., dielectric loss) can be incorporated by the equivalent-circuit model shown in Fig. 1(b). By combining the two models in Fig. 1, frequency-dependent $R, L, G,$ and C can be analyzed. This will be the topic of future work as well as the extension of this equivalent-transmission-line model to multi-conductor transmission lines.

Obviously, frequency-dependent transmission-line parameters will cause a pulse to distort as it propagates down a line. The propagating pulse distortion is a function of the frequency content of the pulse, the length of the line, and the amount of losses in the line. In some situations a simple dc model or even a lossless transmission-line model is adequate for analyzing signal integrity. But, in general, one cannot say when simple models can be used and when a more detailed model is required. Future work is needed in order to lay out some guidelines about when simple transmission-line models can be used to analyze pulse propagation on lossy lines.

Acknowledgment

The authors wish to thank D. F. Williams, N. Morgan, and D. Walker of NIST for the measured data.

References

[1] N. I. Gumerova, B. V. Efimov, and M. V. Kostenko, "Computation of wave deformation due to atmospheric discharges in transmission line," *Elektrich.*, no. 6, pp. 58–61, 1980. in Russian.

[2] D. B. Kuznetsov and J. E. Schutt-Aine, "Optimal transient simulation of transmission lines," *IEEE Trans. Circuits Syst. I*, vol. 43, pp. 110–121, Feb. 1996.

[3] D. B. Kuznetsov, "Efficient circuit simulation of nonuniform transmission lines," *IEEE Trans. Microwave Theory Tech.*, vol. 46, pp. 546–550, May 1998.

[4] K. M. Coperich, A. C. Cangellaris, and A. E. Ruehli, "Rigorous modeling of the frequency dependence of ohmic losses in high-speed electrical interconnections," in *Proc. IEEE Int. Symp. Electromagnetic Compatibility*, Washington, DC, Aug. 21–25, 2000, pp. 301–306.

[5] F. Y. Chang, "Waveform relaxation analysis of nonuniform lossy transmission lines characterized with frequency-dependant parameters," *IEEE Trans. Circuits Syst.*, vol. 38, pp. 1484–1500, Dec. 1991.

[6] C. S. Yen, Z. Fazarinc, and R. L. Wheeler, "Time-domain skin-effect model for transient analysis of lossy transmission lines," *Proc. IEEE*, vol. 70, pp. 750–757, July 1982.

[7] P. Silvester, "Model network theory of skin effect in flat conductors," *Proc. IEEE*, vol. 54, pp. 1147–1151, Sept. 1966.

[8] S. Kim and D. P. Neikirk, "Compact equivalent circuit model for the skin effect," in *Proc. 1996 IEEE-MMT-S Intern. Microwave Symp.*, San Francisco, CA, June 17–21, 1996, pp. 1815–1818.

[9] ——, "Time domain multiconductor transmission line analysis using effective internal impedance," in *Proc. IEEE 6th Topical Meeting on Electrical Performance of Electronic Packaging (EPEP'97)*, San Jose, CA, Oct. 27–29, 1997.

[10] H. A. Wheeler, "Formulas for the skin effect," *Proc. IREE*, vol. 30, pp. 412–424, Sept. 1942.
[11] C. R. Paul, *Analysis of Multiconductor Lines*. New York: Wiley, 1994.
[12] J. A. Roden, C. R. Paul, W. T. Smith, and S. D. Gedney, "Finite-different, time-domain anaalysis of lossy transmission lines," *IEEE Trans. Electromagn. Compat.*, pp. 15–24, Feb. 1996.
[13] D. F. Williams, J. E. Rogers, and C. L. Holloway, "Multicondutor transmission line characterization: Representation, approximations, and accuracy," *IEEE Trans. Microwave Theory Tech.*, vol. 47, pp. 403–409, Apr. 1999.
[14] C. Gordon, T. Blazeck, and R. Mittra, "Time-domain simulation of multiconductor transmission lines with frequency-dependent losses," *IEEE Trans. Computer-Aided Design*, vol. 11, pp. 1372–1387, Nov. 1992.
[15] Y. Eo and W. R. Eisenstadt, "High-speed VLSI interconnect modeling based on S-parameter measurements," *IEEE Trans. Comp., Hybrids, Manuf. Technol.*, vol. 16, pp. 555–562, Aug. 1993.
[16] N. S. Nahman and D. R. Holt, "Transient analysis of coaxial cables using the skin effects approximation $A + B\sqrt{s}$," *IEEE Trans. Circuit Theory*, vol. 19, pp. 443–450, Sept. 1972.
[17] D. F. Williams and C. L. Holloway, "Transmission-line parameter approximation for digital simulation," *IEEE Trans. Electromagn. Compat.*, vol. 43, pp. 466–470, Nov. 2001.
[18] A. R. Djordjevic, T. K. Sarkar, and R. F. R. Harrington, "Analysis of lossy transmission lines with arbitrary nonlinear terminal networks," *IEEE Trans. Microwave Theory Tech.*, pp. 660–666, June 1986.
[19] R. E. Matick, *Transmission Lines for Digital and Communication Networks*. New York: IEEE Press, 1969.
[20] P. C. Marnusson, G. C. Alexander, and V. K. Tripathi, *Transmission Lines and Wave Propagation*. Boca Raton, FL: CRC Press, 1992.
[21] C. R. Paul, *Analysis of Multiconductor Transmission lines*. New York: Wiley, 1994.
[22] C. T. A. Johnk, *Engineering Electromagnetic Fields and Waves*. New York: Wiley, 1975.
[23] C. L. Longmire and K. S. Longley, "Time Domain Treatments of Media with Frequency Dependent Electrical Parameters," Mission Research Corporation, Santa Barbara, CA, MRC-N-1, DNA 3167F, Mar. 1971.
[24] J. D. Hoffman and H. G. Pfeiffer, "Theory of dielectric relaxation for a single-axis rotator in a crystalline field," *J. Chem.Phys.*, vol. 22, no. 1, pp. 132–141, 1954.
[25] J. I. Lauritzen, "Analysis of dielectric loss in two area addition compounds: The hindered single axis polar rotator," *J. Chem.Phys.*, vol. 28, no. 1, pp. 118–131, 1958.
[26] C. L. Holloway, P. Mckenna, and D. A. Steffen, "Finite-difference time-domain modeling for field predictions inside rooms," in *Proc. 1997 IEEE Int. Symp. Elctromanetic. Compatibility*, Austin, TX, Aug. 18–22, 1997, pp. 60–65.
[27] C. L. Holloway, P. Mckenna, and R. T. Johnk, "The effects of gaps in ferrite tiles on both absorber and chamber performance," in *Proc. 1999 IEEE Int. Symp. Elctromanetic. Compatibility*, Seattle, WA, Aug. 2–6, 1999, pp. 239–244.
[28] B. Gustavsenabd and A. Semlyen, Rational approximation of frequency-domain responses by fitting, presented at the IEEE/PES Winter Meeting, New York, 1997.
[29] D. F. Williams and R. B. Marks, "Transmission line capacitance measurement," *IEEE Microwave Guided Wave Lett.*, pp. 243–245, Sept. 1991.
[30] R. B. Marks and D. F. Williams, "Characteristic impedance determination using propagation constant measurement," *IEEE Microwave Guided Wave Lett.*, pp. 141–143, June 1991.
[31] C. L. Holloway and E. F. Kuester, "Edge shape effects and quasiclosed form expressions for the conductor loss of microstrip lines," *Radio Science*, vol. 29, no. 3, pp. 539–559, 1994.
[32] ——, "A quasiclosed form expression for the conductor loss of CPW lines, with an investigation of edge shape effects," *IEEE Trans. Microwave Theory Tech.*, vol. 43, pp. 2695–2701, Dec. 1995.
[33] C. L. Holloway, "Expressions for the loss of stripline and coplanar strip (CPS) structures," *Microwave Opt. Technol. Lett.*, vol. 25, no. 3, pp. 162–167, 2000.
[34] H. A. Wheeler, "Transmission-line properties of a strip on a dielectric sheet on a plane," *IEEE Trans. Microwave Theory Tech.*, vol. 25, pp. 631–647, Aug. 1977.
[35] C. R. Paul, private communication, June 2000.
[36] E. F. Kuester, "Accurate approximations for functions appearing in the analysis of microstrip," *IEEE Trans. Microwave Theory Tech.*, vol. 32, pp. 131–133, 1984.
[37] A. U. Bhobe, C. L. Holloway, and M. Piket-May, "Meander delay line challenge problem: A comparison using FDTD, FEM, and MOM," in *Proc. IEEE 2001 Int. Symp. Electromagnetic Compatibility*, Montreal, QC, Canada, Aug. 13–17, 2001, pp. 805–810.

Alberto Scarlatti was born in Rome, Italy, in 1974. He received the electrical engineering degree, cum laude, from the University of Rome "La Sapienza" in 1998, presenting a thesis work on electromagnetic radiated emission from modal current components on multiconductor transmission lines. Since,1999 heis working toward the Ph.D. degree in electrical engineering at the same university.

During the second semester of the year 2000, he was a Visiting Researcher at the University of Colorado, Boulder and at the National Institute of Standards and Technology (NIST) where he worked on the numerical analysis of scattering problems with FDTD techniques. Since 1999, his research activity is mainly in the field of electromagnetic compatibility and includes the simulation and modeling of multiconductor networks and the analysis of crosstalk and radiated electromagnetic emissions.

Christopher L. Holloway (S'86–M'92) was born in Chattanooga, TN, on in1962. He received the B.S. degree from the University of Tennessee, Chattanooga in 1986, and the M.S. and Ph.D. degrees from the University of Colorado, Boulder in 1988 and 1992, respectively, both in electrical engineering.

During 1992, he was a Research Scientist with Electro Magnetic Applications, Inc., Lakewood, CO. His responsibilities included theoretical analysis and finite-difference time-domain modeling of various electromagnetic problems. From the fall of 1992 to 1994, he was with the National Center for Atmospheric Research (NCAR), Boulder, CO. While at NCAR, his duties included wave propagation modeling, signal processing studies, and radar systems design. From 1994 to 2000, he was with the Institute for Telecommunication Sciences (ITS) at the U.S. Department of Commerce, Boulder, Co., where he was involved in wave-propagation studies. Since 2000, he has been with the National Institute of Standards and Technology (NIST), Boulder, CO, where he works on electromagnetic theory. He is also on the Graduate Faculty at the University of Colorado at Boulder. His research interests include electromagnetic field theory, wave propagation, guided wave structures, remote sensing, numerical methods, and EMC/EMI issues.

Dr. Holloway was awarded the 1999 Department of Commerce Silver Medal for his work in electromagnetic theory and the 1998 Department of Commerce Bronze Medal for his work on printed circuit boards. He is a member of Commission A of the International Union of Radio Science and is an Associate Editor on propagation for the IEEE TRANSACTIONS ON ELECTROMAGNETIC COMPATIBILITY.